Korean J. Chem. Eng., 39(7), 1762-1767 (2022)
DOI: 10.1007/s11814-022-1097-0

pISSN: 0256-1115
eISSN: 1975-7220

Effect of the physicochemical properties of SiO_2 on performance of supported metallocene catalyst

Hyeok Jae Yoo and Young Soo Ko[†]

Department of Chemical Engineering, Kongju National University, 1223-24 Cheonan-daero,
Seobuk-gu, Cheonan 31080, Korea

(*Received 11 December 2021 • Revised 22 February 2022 • Accepted 2 March 2022*)

Abstract−The effect of the calcination temperature of SiO_2 on ethylene polymerization behavior was studied with supported metallocene catalysts. The concentration of hydroxyl group on the SiO_2 surface was measured through FT-IR, thermogravimetry, and trimethylaluminium titration method. In addition, physical properties such as particle morphology, surface area, and pore characteristics were analyzed through BET, and SEM. $(n\text{-}BuMeCp)_2ZrCl_2$ was supported on the SiO_2, which was calcined at different temperatures in the range of 100 and 900 °C. The resulting supported catalyst was applied to ethylene homopolymerization and ethylene-1-hexene copolymerization at 80 °C and 20 bar, showing that the lower calcination temperature resulted in higher activity due to the larger Zr and Al loadings.

Keywords: Metallocene Catalyst, SiO_2, Support, Polyethylene, Polymerization

INTRODUCTION

Metallocene catalyst exhibits unique polymerization performances that are differentiated from Ziegler-Natta and Phillips catalysts due to its single-site feature [1]. When a cocatalyst such as methylaluminoxane (MAO) or borane compound is used, the central metal of the metallocene precursor is activated to the cation, resulting in that olefin polymerization can occur [2,3]. Theoretically, all the properties of the active sites are the same, rendering them possible to precisely control the molecular structure of the polymer during polymerization, and to be suitable for controlling the physical properties of the polymer.

Metallocene has been attractive for its superior performance to that of conventional catalysts, but two major problems have emerged. One is reactor fouling and sheeting during homogeneous polymerization [4-7]. Second, an excessive amount of expensive MAO cocatalyst is required for metallocene activation [8,9]. In particular, the former problem is a factor that greatly reduces process efficiency and must be solved for commercialization. To overcome this problem, a method of preparing a heterogeneous catalyst by supporting a metallocene precursor on an appropriate support has been developed and commercialized. Silica, alumina, zeolite, clay minerals, graphene, etc. have been employed as support [10-19]. Silica has been a major support material due to its excellent thermal stability, mechanical strength, surface area, and economic feasibility.

The physicochemical properties of the SiO_2, such as particle size, mechanical strength, surface area, and surface properties, could have a great influence on operability in the polymerization process. It has been reported that polymers grow from supported metallocene particles via fragmentation process during polymerization [20-22]. If the mechanical strength of silica support is too weak, the catalyst particles might be broken to be fine particles during the fragmentation process, causing severe process problems. Therefore, it is very crucial to select an appropriate support for successful application of supported metallocene to the commercial processes of olefin polymerization.

SiO_2 possesses a certain amount of moisture due its large surface area and pore volume. Since metallocene is rapidly deactivated when it contacts with oxygen or moisture, its content inside SiO_2 can influence catalyst activity. Therefore, it is necessary to perform calcination to remove moisture and to control OH content inside the silica [23-25]. However, there have been few studies on the effect of the characteristics of SiO_2 on polymerization performance. SiO_2 has been supplied to polyolefin producers from silica producers without information on the effect of calcination temperature. The effect of calcination temperature of SiO_2 on its physicochemical properties and polymerization should be studied to understand and improve the performance of supported metallocene.

In this study, the effect of the calcination temperature of SiO_2 on PE polymerization behavior was studied with supported metallocene in detail. SiO_2 was calcined at different temperature (100, 200, 400, 550, 700 and 900 °C) for over ten hours. The concentration of silanol group on the silica surface according to the calcination temperature was measured with both thermogravimetry (TG) analysis and trimethylaluminium (TMA) titration. FT-IR analysis was also performed to investigate the structure of silanol on the silica surface depending on calcination temperature. BET analysis was performed to determine the surface area and pore diameter of SiO_2. Finally, bis(1-methyl-3-butylcyclopentadienyl)zirconium dichloride ($(n\text{-}BuMeCp)_2ZrCl_2$) was supported on SiO_2 with MAO, and then PE polymerizations were carried out with the resulting supported $(n\text{-}BuMeCp)_2ZrCl_2$.

[†] To whom correspondence should be addressed.
E-mail: ysko@kongju.ac.kr

EXPERIMENTAL

1. Materials

ES70 (PQ Corporation) silica was pretreated by calcining at each temperature for ten hours under nitrogen flow and stored in a glove box. Nitrogen gas (Daedeok gas, 99.999%) and ethylene gas (World Enersys, 99.9999%) were passed through RIDOX (Fisher) and 5A/13X molecular sieve columns to remove oxygen and moisture. Toluene (J.T. Baker, HPLC grade) and hexane (J.T. Baker, HPLC grade) were used after purification by reflux distillation with sodium metal and benzophenone. The metallocene precursor bis(1-methyl-3-butylcyclopentadienyl)zirconium dichloride($(n\text{-}BuMeCp)_2ZrCl_2$, 98%, s-PCI) was used without purification. Methylaluminoxane (MAO, 10 wt% in toluene, Grace) used as a cocatalyst without further purification. Triethylaluminium (TEAL, 1.0 M in hexane, Aldrich) used as a scavenger during polymerization was used without additional treatment, and 1-hexene (Acros Organics, 97%), a comonomer for copolymerization was purified with a 3 Å molecular sieve.

2. Characterization of SiO_2 According to the Calcination Temperature

FT-IR (Thermo Fisher Scientific, Nicolet 6700) analysis was performed to investigate the chemical groups of silica support. After the pellet was mounted on an in-situ IR cell, it was vacuumed at room temperature for one hour before analysis. Measurements were made with a resolution of 4 cm^{-1} and 32 scans in the wavenumber range of 4,000 to 400 cm^{-1}. Thermogravimetric analysis confirmed the concentration of the silanol group according to the silica calcination temperature. The equipment used was SDT Q600 (TA Instruments), and the analysis was performed while flowing nitrogen at 100 mL/min. A sample was heated from room temperature to 1,200 °C at a rate of 5 °C/min to measure the weight loss [16]. Titration using TMA reagent was performed to quantify the concentration of hydroxyl groups on the silica surface according to the calcination temperature [23]. The OH group on silica surface reacted with one molecule of TMA to generate CH_4 gas. The titration method proceeded as follows: after 0.3 g of SiO_2 was weighed in a flask, it was purged with nitrogen gas for 1 hour. 10.0 mL of toluene was added to the flask, and 1.0 mmol of the TMA solution was added thereto, followed by stirring. Titration was performed at room temperature, ranging from a minimum of 1 hour to a maximum of 3 hours and terminated when gas generation no longer occurred. FE-SEM analysis was performed using MIRA LMH (TESCAN) to observe the morphology of silica particles. The surface area and pore characteristics according to the silica calcination temperature were measured using ASAP2020 (Micromeritics). The sample was heated from room temperature to 150 °C at a rate of 10 °C/min while vacuuming. The surface area was calculated using the Brunauer-Emmett-Teller (BET) method, and the pore diameters were calculated according to the BJH (Barrett-Joyner-Halenda) method.

3. Preparation and Analysis of Supported Metallocene

In a flask, 0.1 mmol of metallocene was weighed, and 10 mL of toluene was added. After slowly adding 8.0 mmol of MAO to this, the mixture was stirred at room temperature for 1 hour. In the second flask, 1.0 g of SiO_2 was weighed, and 20 mL of toluene was added. Then, a mixture of metallocene and MAO was added dropwise, and reacted with mild stirring at room temperature for 1 hour. After the reaction was completed, the supernatant was removed and washed with toluene several times to remove unreacted substances. It was vacuum dried at 40 °C for about two hours to obtain a powdery catalyst.

ICP-MS (Perkin Elmer, NEXION-350X) analysis was performed to confirm the amount of Zr and Al metal supported on the prepared catalyst. Sample preparation was performed using Titan MPS (Perkin Elmer). SEM-EDS analysis was performed using MIRA LMH(TESCAN) to confirm the distribution of Si, Zr, and Al elements of the prepared catalyst. As an X-ray detector, an Xflash 4010 (Bruker) with 125 eV resolution was used.

4. Ethylene Polymerization

Ethylene polymerization was carried out in a 250 mL autoclave reactor equipped with a magnetic stirrer. A polymerization solvent was prepared by adding 140 mL of hexane and 0.5 mmol of TEAL using a scavenger to a 500 mL glass bottle. During copolymerization, 1.4 mL of 1-hexene was additionally added. After purging the reactor with ethylene and nitrogen gas several times, a solvent was added at 50 °C. At a reactor temperature of 70 °C, the prepared supported catalyst was injected into reactor. With feeding ethylene gas to the reactor, the polymerization was carried out at 80 °C and 20 bar for 1hr. After polymerization, ethanol was added to deactivate the catalyst.

RESULTS AND DISCUSSION

1. Characterization of Silica Support

TG analysis of SiO_2 which was calcined at different temperature showed that there were two regions in which the sample weight decreased as the temperature increased as shown in Fig. 1. The moisture physically adsorbed on the silica surface was removed at around 100 °C and the weight of uncalcined silica decreased significantly. At above 100 °C the weight loss gradually decreased as the calcination temperature increased. In the second region (above 200 °C), one molecule of H_2O was released from two adjacent silanol groups, and isolated, geminal, and vicinal silanol groups were

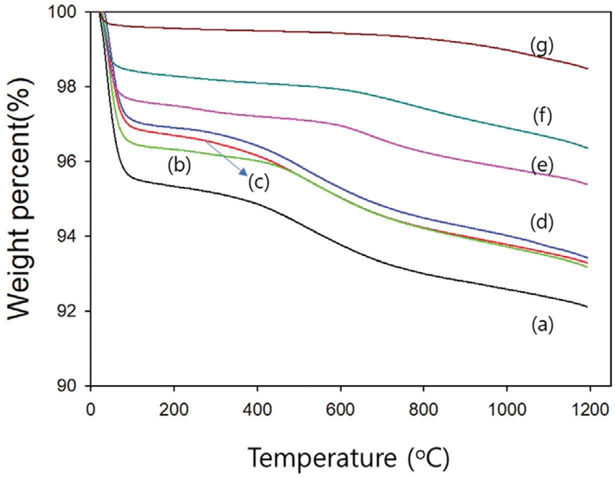

Fig. 1. TG curves of (a) uncalcined silica, and silica calcined at (b) 100, (c) 200, (d) 400, (e) 550, (f) 700 and (g) 900 °C.

Table 1. Analysis of hydroxyl group content on silica surface

Silica calcined temperature (°C)	TGA		TMA titration	
	Hydroxyl group contents (mmol/g-SiO_2)	Hydroxyl group contents (OH/nm^2)	Hydroxyl group contents (mmol/g-SiO_2)	Hydroxyl group contents (OH/nm^2)
100	4.16	9.65	2.78	6.45
200	4.23	9.54	2.54	5.72
400	3.80	8.64	2.30	5.23
550	2.71	6.10	2.04	4.60
700	2.50	4.79	1.67	3.20
900	1.40	2.93	0.90	1.89

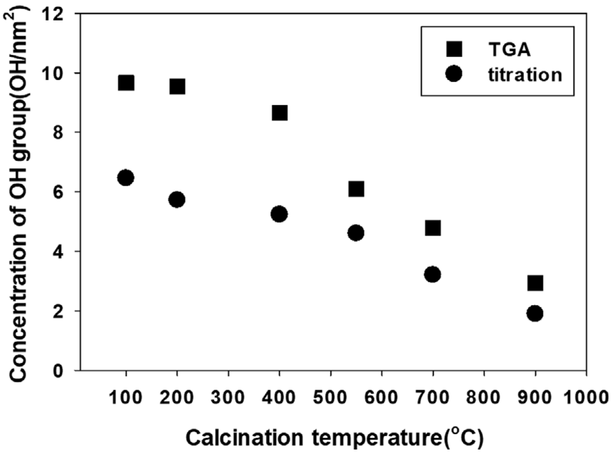

Fig. 2. OH group content on silica surface measured by TMA titration and TG analysis.

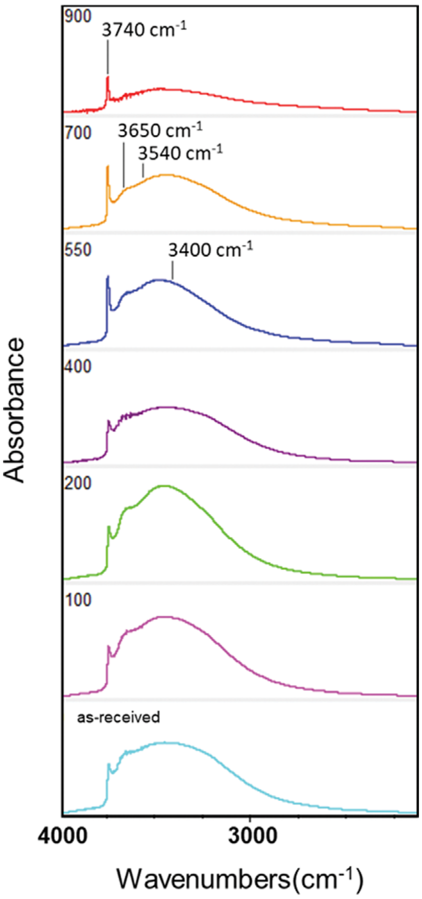

Fig. 3. FT-IR spectra of silica calcined at different temperatures.

reported to be converted into siloxane group [26]. On the assumption that the weight lost in the second region resulted from that of hydroxyl groups on the silica surface, the concentration of hydroxyl groups present in 1 g of SiO_2 could be calculated using the following equation [21]. The calculated values are summarized in Table 1.

$$\text{OH contents (mol/g-silica)} = \frac{2(\text{Weight loss from } 200\,^{\circ}\text{C to } 1{,}200\,^{\circ}\text{C, \%})}{100 * 18\ \text{g/mol}}$$

On the other hand, the hydroxyl group concentration measurement using TMA titration method also decreased as the calcination temperature increased. The hydroxyl group concentration by TMA titration method was less than that that of TG method by about 1 mmol/g- SiO_2 (Fig. 2) for all calcination temperatures. This can arise from the fact that TMA did not diffuse deep into the micropore of SiO_2 during the titration and it mainly reacted with hydroxyl groups present inside the pore, which was larger than TMA molecule. Since the supported metallocene is prepared by diffusion of metallocene molecule, which is similar to the titration method, the OH concentration measured by the TMA titration method could be more reasonable for the immobilization of metallocene.

FT-IR spectra were obtained as shown in Fig. 3. The peak at 3,740 cm^{-1} is assigned to be an isolated silanol group which plays an important role in binding metallocene and cocatalyst to the surface of SiO_2 [27]. The peak intensity at 3,740 cm^{-1} gradually increased with increasing in calcination temperature. The broad peak in the range of 3,650 cm^{-1} and 3,540 cm^{-1} corresponds to inaccessible silanol and vicinal silanol group of SiO_2, respectively. It has been reported that most of reactants could not have access to inaccessible silanol, and particularly for larger molecules [28]. The peak intensities of inaccessible silanol and vicinal silanol were weak and difficult to identify due to interference, but they gradually decreased with the calcination temperature. Similarly, the peak intensity at the 3,400 cm^{-1} assigned to physically adsorbed water decreased with increasing the calcination temperature. Taking the results of TGA, TMA titration, and FT-IR analysis into consideration, most of the physically adsorbed moisture was removed at the silica calcination temperature of about 100 °C. At higher temperature above 200 °C,

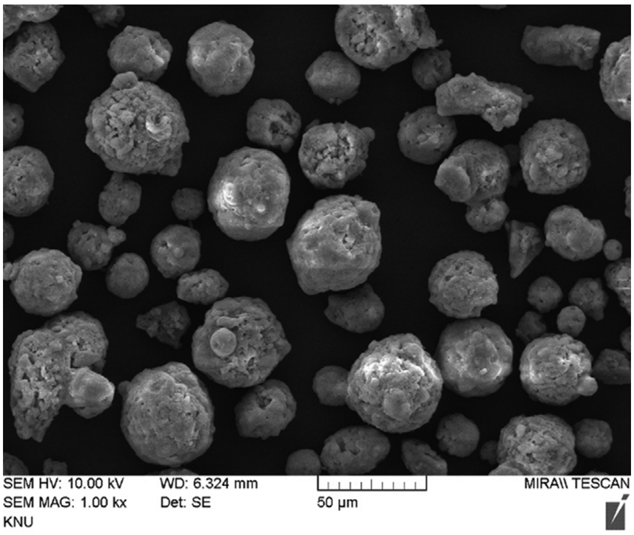

Fig. 4. SEM images of ES70 silica.

it was confirmed that dehydroxylation occurred through converting geminal and vicinal silanol groups to isolated silanol and finally to siloxane structure.

Fig. 4 shows the result of SEM analysis and SiO_2 had spherical shape. As shown in Fig. 5, the average surface area and pore diameter were in the range of 275 m^2/g-SiO_2, and about 20 nm, respectively. ES70 silica showed little change in surface area and pore properties regardless of the calcination temperature in the range of 100 and 900 °C, meaning that the pore structure of SiO_2 was quite stable below 900 °C.

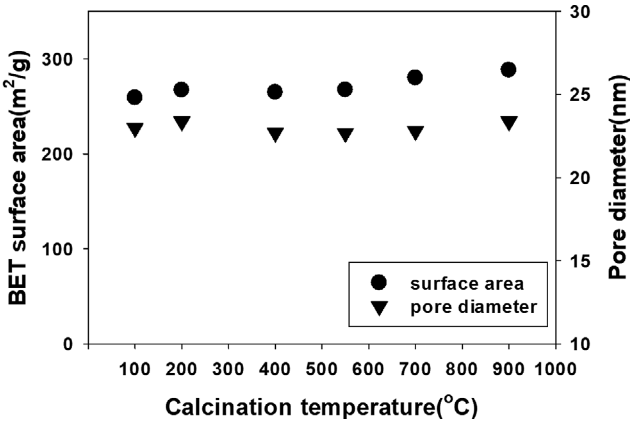

Fig. 5. BET surface area and pore diameter of silica.

2. Characteristics Analysis of Supported Metallocene Catalyst and PE Polymerization Results

Fig. 6 shows SEM-EDS images of supported metallocene which was prepared with SiO_2 calcined at 100 °C. Metallocene and MAO were evenly distributed on the silica support in appearance. Table 2 shows the loading amount of Zr and Al in the supported metallocene. Both Zr and Al loadings were almost constant at the calcination temperatures of 100 and 400 °C. However, both Zr and Al loading were decreased by more than 20% above 700 °C. This might result from the lower OH content at high calcination temperature.

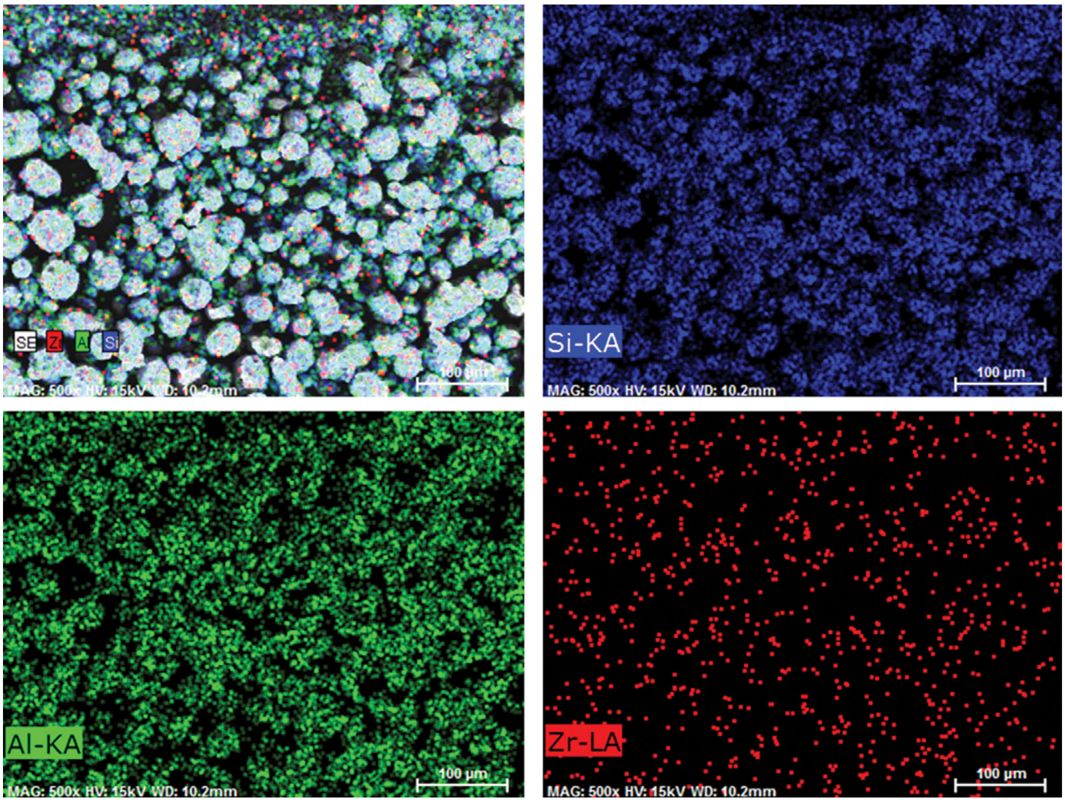

Fig. 6. SEM-EDS images of supported metallocene catalyst.

Table 2. Results on ethylene polymerization with SiO_2 supported $(n\text{-}BuMeCp)_2ZrCl_2$ catalyst

Silica calcined temperature (°C)	Zr content (μmol/g-cat)	Al content (mmol/g-cat)	Al/Zr molar ratio	Activity (kg-PE/g-cat*h)	
				Homopolymerization	Copolymerization
100	51.1	5.5	107	1.91	2.61
400	55.4	5.4	97	1.51	2.51
700	44.0	4.7	107	1.29	1.73
900	37.7	4.3	114	0.91	1.32

Polymerization condition: ethylene pressure=20 bar, temperature=80 °C, TEAL in feed=0.5 mmol, catalyst feed=10 mg, time=1 h

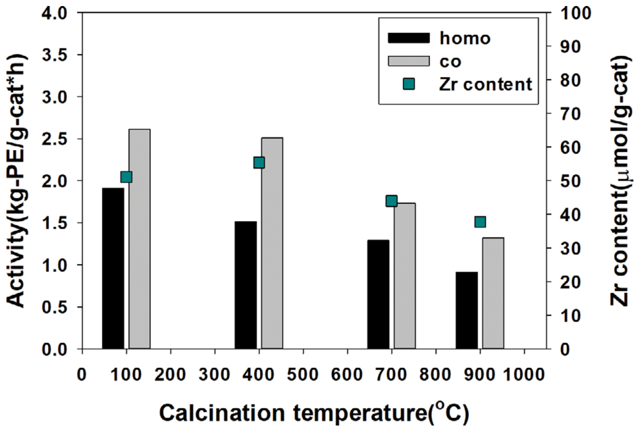

Fig. 7. Homo and copolymerization activity according to silica calcination temperature.

The OH group seemed to be crucial to control Zr and Al loadings in supported metallocene because the covalent bonding between SiO_2 surface and two complexes can be formed via OH group.

Both homo- and copolymerization activities with supported metallocene are shown in Table 2 and Fig. 7. The activity was strongly dependent on the calcination temperature, and it decreased as the calcination temperature increased. The Zr and Al loadings were dependent on the calcination temperature and decreased as it increased, resulting in that the polymerization activity decreased due to lower Zr and Al loadings of supported metallocene. The highest activity was shown with supported metallocene, which SiO_2 was calcined at 100 °C. At above 400 °C it decreased gradually down to 0.91 and 1.32 kg-PE/g-cat hr. The OH group provides attaching the metallocene catalyst or MAO cocatalyst to the silica surface through a covalent bond. In the study, the OH group concentration on the surface decreased as the calcination temperature of silica increased, so it can be inferred that the catalyst loading amount decreased as shown in Table 2. As shown in Fig. 2, the Zr and Al loadings decreased as the calcination temperature increased, resulting in lower polymerization activity at higher calcination temperature.

Judging from the TG curve as shown in Fig. 1, most of the moisture physically adsorbed to silica was removed at around 100 °C or higher. Uncalcined silica contains moisture, which is a catalyst poison, but silica calcined at 100 °C has the most of physisorbed moisture removed and only OH groups exist on the silica surface. The water content is minimal and the OH group is maximal at 100 °C of calcination temperature, so it could show the highest activity.

CONCLUSIONS

The effect of the calcination temperature of SiO_2 on PE polymerization behavior was investigated in detail. The OH content on the SiO_2 was measured with both TG and TMA titration methods, giving lower values of OH content for TMA titration. FT-IR showed that the dehydroxylation of SiO_2 occurred through converting geminal and vicinal silanol groups to isolated silanol and finally to siloxane structure. The polymerization results suggested that the activity was dependent on the calcination temperature of SiO_2, and it decreased as the calcination temperature increased. The concentration of hydroxyl group on SiO_2 surface seemed to be crucial to optimize the performance of supported metallocene since it controlled Zr and Al loadings of the supported one.

ACKNOWLEDGEMENTS

This work was supported by a National Research Foundation of Korea (NRF) grant funded by the Korean government (MSIP) (2016R1D1A1B01009941) and by the research grant of the Kongju National University in 2020.

REFERENCES

1. W. Kaminsky and A. Laban, *Appl. Catal. A Gen.*, **222**(1-2), 47 (2001).
2. W. Kaminsky, *J. Chem. Soc. - Dalt. Trans.*, 9, 1413 (1998).
3. W. Kaminsky and M. Arndt, *Adv. Polym. Sci.*, **127**, 143 (1997).
4. B. Heurtefeu, C. Bouilhac, É. Cloutet, D. Taton, A. Deffieux and H. Cramail, *Prog. Polym. Sci.*, **36**(1), 89 (2011).
5. G. Fink, B. Steinmetz, J. Zechlin, C. Przybyla and B. Tesche, *Chem. Rev.*, **100**(4), 1377 (2000).
6. M. A. Bashir, V. Monteil, C. Boisson and T. F. L. McKenna, *React. Chem. Eng.*, **2**(4), 521 (2017).
7. E. M. Carnahan and G. B. Jacobsen, *Cattech*, **4**(1), 74 (2000).
8. H. G. Alt, *Dalt. Trans.*, 20, 3271 (2005).
9. E. Zurek and T. Ziegler, *Prog. Polym. Sci.*, **29**(2), 107 (2004).
10. T. Tayano, H. Uchino, T. Sagae, K. Yokomizo, K. Nakayama, S. Ohta, H. Nakano and M. Murata, *Macromol. React. Eng.*, **11**(2), 1 (2017).
11. M. Stürzel, Y. Thomann, M. Enders and R. Mülhaupt, *Macromolecules*, 47(15), 4979 (2014).
12. J. H. Yim, J. S. Lee and Y. S. Ko, *Polymer*, **39**(1), 169 (2015).
13. J. S. Lee, J. H. Yim, J. K. Jeon and Y. S. Ko, *Catal. Today*, **185**(1), 175 (2012).
14. A. C. Cariño, S. J. Park and Y. S. Ko, *Appl. Chem. Eng.*, **29**(4), 461

(2018).

15. S. Y. Lee and Y. S. Ko, *J. Nanosci. Nanotechnol.*, **13**(6), 4401 (2013).
16. J. S. Lee and Y. S. Ko, *J. Mol. Catal. A Chem.*, **386**, 120 (2014).
17. J. D. Encarnacion, S. J. Park and Y. S. Ko, *Korean J. Chem. Eng.*, **37**(2), 380 (2020).
18. J. Celedonio, J. S. Lee and Y. S. Ko, *Appl. Chem. Eng.*, **25**(4), 396 (2014).
19. Y. S. Ko, J. S. Lee, J. H. Yim, J. K. Jeon and K. Y. Jung, *J. Nanosci. Nanotechnol.*, **10**(1), 180 (2010).
20. X. Zheng, M. Smit, J. C. Chadwick and J. Loos, *Macromolecules*, **38**(11), 4673 (2005).
21. S. Ek, A. Root, M. Peussa and L. Niinistö, *Thermochim. Acta*, **379**(1-2), 201 (2001).
22. A. R. Albunia, F. Parades and D. Jeremic, *Multimodal polymers with supported catalysts*, Springer, New York (2019).
23. R. Van Grieken, G. Calleja, D. Serrano, C. Martos, A. Melgares and I. Suarez, *Polym. React. Eng.*, **11**(1), 17 (2003).
24. M. Atiqullah, M. N. Akhtar, A. A. Moman, A. H. Abu-Raqabah, S. J. Palackal, H. A. Al-Muallem and O. M. Hamed, *Appl. Catal. A Gen.*, **320**, 134 (2007).
25. M. A. Bashir, T. Vancompernolle, R. Gauvin, L. Delevoye, N. Merle, V. Monteil, M. Taoufik, T. F. L. McKenna and C. Boisson, *Catal. Sci. Technol.*, **6**(9), 2962 (2016).
26. R. Mueller, H. K. Kammler, K. Wegner and S. E. Pratsinis, *Langmuir*, **19**(1), 160 (2003).
27. J. P. Gallas, J. M. Goupil, A. Vimont, J. C. Lavalley, B. Gil, J. P. Gilson and O. Miserque, *Langmuir*, **25**(10), 5825 (2009).
28. C. G. Armistead, A. J. Tyler, F. H. Hambleton, S. A. Mitchell and J. A. Hockey, *J. Phys. Chem.*, **73**(11), 3947 (1969).